

COMPARISONS OF CEM PREDICTIONS TO IR IMAGES OF EM FIELDS FOR COMPLEX SYSTEMS

John Norgard
US AFRL/RRS(SNRT)
Rome, NY, USA

Randall Musselman
US Air Force Academy, DFEC
Colorado Springs, CO, USA

Irina P. Kasperovich and Andrew L. Drozd
ANDRO Computational Solutions, LLC
Beeches Technical Campus
7902 Turin Road, Ste. 2-1
Rome, NY, USA

ABSTRACT

An infrared (IR) measurement technique, based on thermal principles, is presented to independently validate and verify (V&V) numerical codes used for computational electromagnetic (CEM) field predictions. This technique is applied to scattering and to complex systems such as antennas on aircraft. The IR technique produces a thermal image of the EM field over any two-dimensional area, usually a plane, proportional to the intensity of the incident EM field being measured. This IR image can be compared to the predicted image of the field calculated with a numerical CEM code over the same plane that was used in the measurements to confirm the field patterns. Precise thermal measurements on metallic scale models of canonical aircraft shapes are made in a controlled anechoic chamber environment. The scattered fields from the model are measured for different test setups. The temperature distribution is converted to field intensity and plotted as a false color image of the field and compared to similar plots from a selected CEM code. The field can also be visualized with this IR method. This is the first step in a progressive approach to compare results of more sophisticated geometries using a suite of CEM codes to confirm the results of the IR measurements and to develop confidence in the complementary measurement and simulation methods.

Keywords: Electromagnetic Scattering, Infrared Measurements, Computational Electromagnetics, Computer Model Verification and Validation, Standards

1.0 Introduction

This paper describes an effort to compare two different methods of predicting the scattered fields for a complex arrangement of canonical objects that resemble an aircraft system. In particular, this effort was to first measure the scattered fields for a selected test article using a horn antenna test setup in conjunction with a novel IR measurement technique. Results were then compared to computer simulations of the same. The test article in this case is a highly simplified, canonical based geometry comprised of perfectly electrically conducting (PEC) plates, a fully-enclosed right circular cylinder and a cone. The physical measurements and computer simulations which are described below focused on irradiating the test article at a few select frequencies in the C-Band with a plane wave at a given polarization and a fixed nose-on position.

It was decided that in order to gain a better understanding of the electromagnetic (EM) phenomenology associated with the geometric scattering, a simplified canonical aircraft representation and limited test conditions would be considered as an initial step. This would provide a baseline understanding of the phenomenology. In the future, the plan is to extend this study using IR and computer simulation techniques to compare the predictions of electromagnetic scattering for more sophisticated systems representing real aircraft at multiple frequencies, different aspect angles, meta materials, etc.

In this paper, an IR measurement technique, based on thermal principles, was used to independently V&V a selected first-principles CEM code, which hybridizes the moment method (MoM) and uniform theory of diffraction (UTD) high-frequency ray tracing techniques. This code was used to predict the far-field scattering from the canonical aircraft

model. The scattered fields were then measured using the IR imaging method. The predicted fields were compared to the measured fields to V&V the code. This is the first in a series of tests to check the numerical codes. Later, the simple canonical model will be replaced by a high-fidelity model of a conventional aircraft, then, later yet, by a stealthy aircraft. The predicted and measured fields scattered by the conventional and stealth aircrafts will also be compared in the future.

Generally, in this process, precise thermal measurements on metallic scale models of canonical aircraft shapes are made in a controlled anechoic chamber environment with a radiating horn antenna to make scattered field measurements around the model. The temperature distribution is converted to field intensity, plotted as a false color image of the field, and compared to similar plots from various CEM codes. The field can also be visualized with this IR method. A selected CEM code is run to confirm the results of the IR measurements to develop confidence in the measurement and simulation methods.

2.0 IR Technique

The IR technique produced thermal images of the EM fields over several planar two-dimensional areas, which were proportional to the intensity of the incident field [1, 2]. The images are presented as 2D contour plots or as 3D relief maps of the relative or absolute intensities of the EM fields being measured. Recall that this IR image is compared to the predicted image of the field calculated with the numerical CEM code over the same plane that was used in the measurements to confirm the field levels. In these comparisons, emphasis is placed on the qualitative similarities and differences (i.e., pattern comparisons), rather than performing a quantitative evaluation of field intensities. This is due to the fact that the false color scales are different between the IR/thermal method and the CEM tool used in the simulations. A technique is being examined to relate the two color bars and scales in order to better accommodate quantitative comparisons.

3.0 IR Setup

The IR measurements were made by placing a thin, lossy (but, low loss) minimally perturbing detector screen in the plane over which the field is to be measured. As the field passes through the screen, some of the EM energy is absorbed by the lossy material of the screen (due to polarization, magnetization, and conduction losses). The absorbed energy causes the temperature of the screen to rise (Joule heating) over the background ambient temperature of the screen. An IR camera is used to measure the temperature distribution created across the screen. The temperature rise, on a pixel-by-pixel basis, is proportional to the local intensity of the EM field incident on the screen. This is a highly non-linear relationship due to the T^4 temperature relationships for black-body radiation. The temperature rise over the background temperature for different screen materials as a function of the intensity of the field incident on the screen has been previously measured at NIST/Boulder to produce a calibration table of the incident field intensity vs. the color temperature of the screen material. Carbon loaded polyimide films are used for these tests that measure the electric field intensity of the EM field incident on the screen. This color table for each screen material (with different carbon loadings) is used to measure the absolute field intensity of the incident field based on the measured color temperature of the screen. The screen that will produce a significant temperature rise over the ambient temperature with the smallest amount of carbon loading, which will cause the smallest perturbation of the field being measured, is selected to measure the incident field.

4.0 IR Measurements

Precise thermal measurements were made in a controlled anechoic chamber environment on a small canonical 1/32 scale model of a selected aircraft. The model consists of a right-cylindrical tube for the fuselage with a conical end cap on the front side and a flat end cap on the back side, as shown in Fig. 1. The wings were constructed from thin, flat, rectangular pieces of metal and were inserted through slots in the fuselage. The horizontal stabilizers were made similar to the wings, but shorter. The vertical stabilizer was triangular shaped and also inserted into a slot in the fuselage.

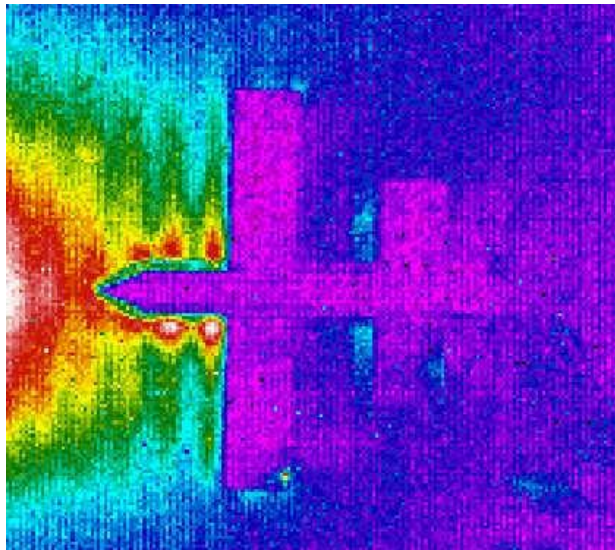
The thin detector screen material was taped onto a flat sheet of Styrofoam. The screen was used to measure the field in the plane of the wings and horizontal stabilizers of the aircraft. An outline of the 1/32 scale model aircraft was cut into the Styrofoam backed screen material and the model was embedded into screen and taped into position. The screen was just under the wings. The screen with the embedded model was placed inside the anechoic chamber on Styrofoam blocks and irradiated at several selected and representative frequencies, viz. from 4 to 8 GHz. The angle-of-incidence was nose-on. The polarization was in the (x-z) plane of the wings. Other angles-of-incidence and polarizations were also tested.

5.0 IR Images

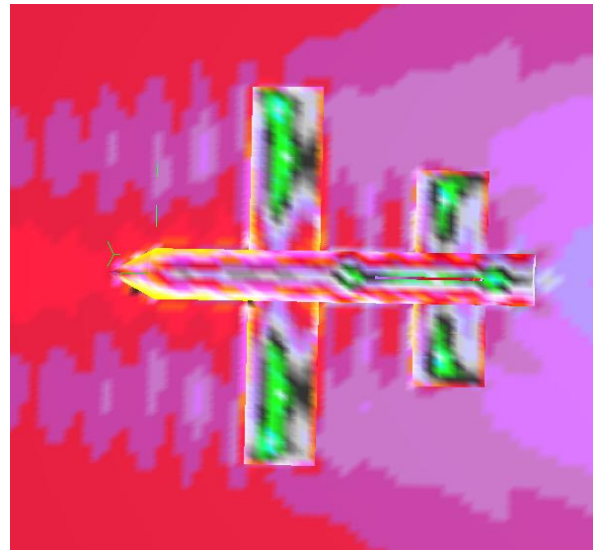
The scattered field was measured around the model. Normally, the resulting temperature distribution is converted to field intensity using a color table. However, in this example, the relative magnitudes were plotted as a contour map, as shown in Fig. 2a at several C-Band frequencies. These images were compared to similar plots from the selected MoM/UTD numerical code that was run for the same case.



Figure 1. Anechoic Chamber and Test Article Setup with Horn Antenna and IR Camera



(a)



(b)

Figure 2. (a) Contour Map Showing Measured Relative Field Magnitudes at 3GHz Using the IR Technique, and (b) Contour Map Showing Relative Co-Pole Field Magnitudes Using a Plane Wave CEM Simulation Technique

6.0 Computer Model

The computer model that was used for the simulations mimicked the basic test setup and conditions that were used for the IR measurements. The geometrical model was identical in form to the canonical model discussed above. It was generated in accordance with the 1/32 scale model dimensions used in the IR measurements. The geometrical objects used to represent the simulation model were all assumed to be PEC.

In the initial runs, both a dipole and a horn source were modeled independently in separate runs. A horizontal electric field polarization was assumed i.e., E-field in the plane of the wings. For accuracy purposes, the horn antenna required a very detailed description of the source feed and the horn structure at the various frequencies of interest. For simplicity and for the purposes of computational efficiency, and since the initial runs were meant to only verify the generalized scattering patterns from a qualitative viewpoint, the simulations focused on using a far-field dipole as the source instead of the horn antenna model. This provided sufficient results which could be used to perform the first-order comparisons to the IR measurements. For example, the predicted scattering at 3 GHz using the plane wave simulation approach is shown in Fig. 2b. Generally, the sampling criterion used in the MoM modeling was 0.1λ where λ is the wavelength at the sample frequency.

7.0 Results and Observations

The original focus of this study was on the frequency of 3 GHz where some interesting scattering phenomena were observed both in the measured and in the simulated models. The structure of the field was visualized with the IR method. For example, the spherical standing wave setup between the horn antenna and the portion of the canonical aircraft where say a phased array radar antenna in the nose may be located, can be easily seen in Fig. 2a (indeed, this is the sort of problem that could be examined in the real world as pertaining to the F-16 Fire Control Radar or other fighter aircraft systems). In addition, the surface wave excited on both sides of the airframe between the tip of the fuselage and the ends of the wings can also be easily identified in the figure (another practical concern). The shadow zone behind the aircraft is also quite evident.

The corresponding simulation results are shown in Fig. 2b, for the horizontal co-pole plane wave case. The same essential features of the scattered wave are present in both the predicted and the measured waves. Note the differences in the color schemes between the measured and the predicted fields, which make the comparisons more difficult to correlate and match. Also, the thermal image is saturated in the standing wave area, so that some of the spherical wave patterns are obscured. Recall that for the initial cases studied, emphasis was on performing a qualitative comparison in order to identify consistent trends or any anomalies with respect to the results of the IR and computer simulation techniques.

The results of Figs. 2a and 2b show good agreement for the standing waves and scattering peaks and nulls in the vicinity of the front cone-cylinder portion of the overall geometry. In the computed model it was also observed that structural resonance currents and resultant standing waves were formed along the cylindrical tube, but are not clearly seen in Fig. 2b due to the relatively high intensity predicted currents and scattered fields. Upon closer examination of the results of Fig. 2b, the standing wave peaks can be more easily observed by changing the perspective of the viewpoint of the computed model.

Other higher frequency cases were also measured and modeled. In these tests, the computer model was changed from a plane wave source to a spherical source. In addition, an attempt was made to better correlate the color scales between the measured and the simulated results.

Figs. 3a and 3b compare the results between the measurement and the simulation for nose-on radiation at 4 GHz. The polarization is in the plane of the wings. The incident wave is clearly seen as a spherical wave. Many of the previously noted features of the scattered field distribution can be noted in the figures. Similarly, Figs. 4a and 4b compare the results between the measurement and the simulation for nose-on radiation at 6 GHz.

Figs. 5a and 5b compare the results between the measurement and the simulation for tail-on radiation at 4 GHz. The polarization, as above, is in the plane of the wings. Again, the incident wave is clearly seen as a spherical wave and, as before, many of the previously noted features of the scattered field distribution can be noted in the figures. Similarly, Figs. 6a and 7b compare the results between the measurement and the simulation for tail-on radiation at 6 GHz.

8.0 Summary

The primary emphasis of this study was on applying an IR measurement technique to independently V&V numerical codes used for CEM field predictions. This was done for a simple canonical metallic scale model of typical aircraft in the Air Force inventory. The immediate goal was to determine if two diverse and independent methods of determining the scattered fields could provide similar results relying on a first-level qualitative comparison. The results obtained were found to be in generally good agreement between the IR and computer simulation techniques, and deemed to be acceptable for the purposes of this initial phase of the study. Further examination of the results of RF measurements of the model will take place in the future and the approach will be expanded to look at more sophisticated aircraft models (e.g., F-16, F-35, etc.). Future studies will also account for multiple frequencies, different aspect angles, and materials. It is also noteworthy to mention that the results of this study will be of much benefit to the IEEE EMC Society Standards Development Committee; in particular, it will benefit the IEEE P1597 Working Group chartered with the development of standards and recommended practices for validating CEM techniques for EMC applications.

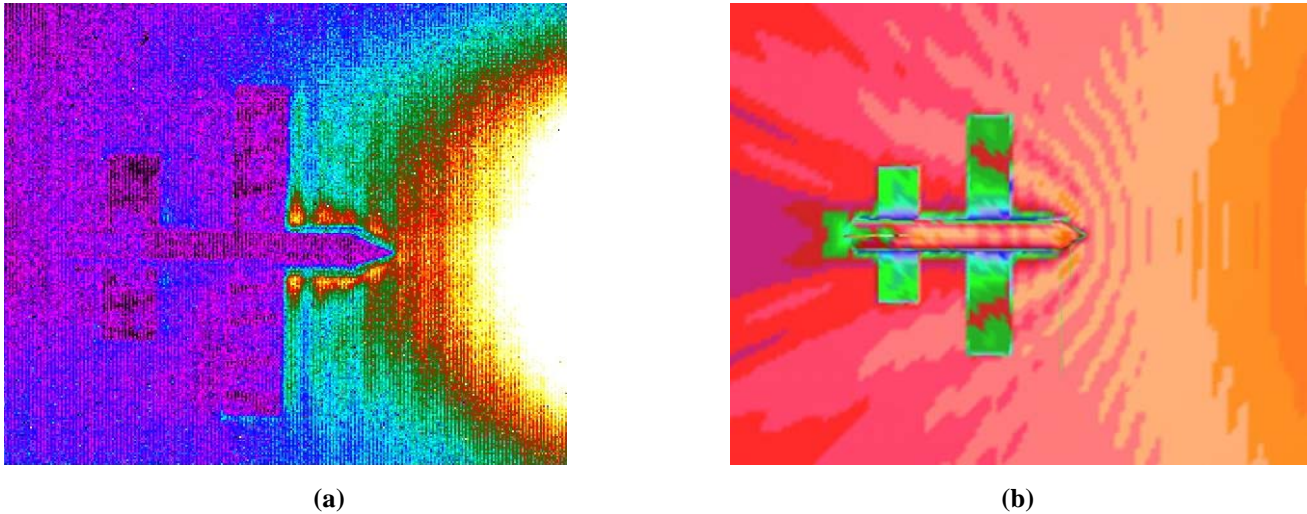


Figure 3. Nose-On at 4GHz (Incident Spherical Wave)
(a) Contour Map Showing Measured Relative Field Magnitudes Using the IR Technique, and
(b) Contour Map Showing Relative Co-Pole Field Magnitudes Using the CEM Simulation Technique

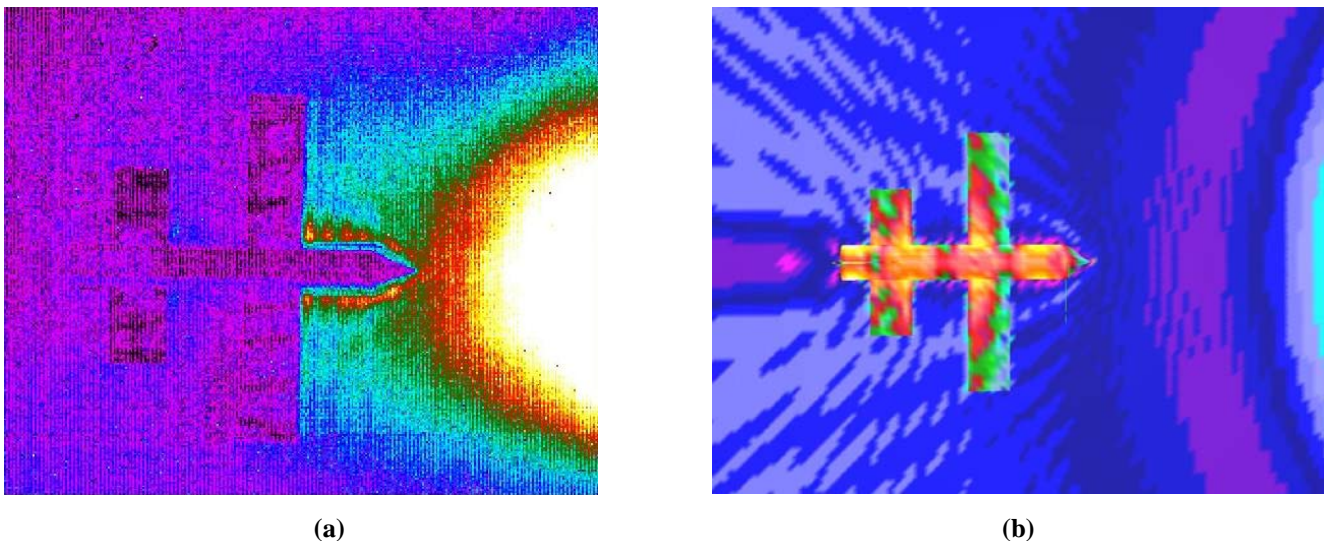
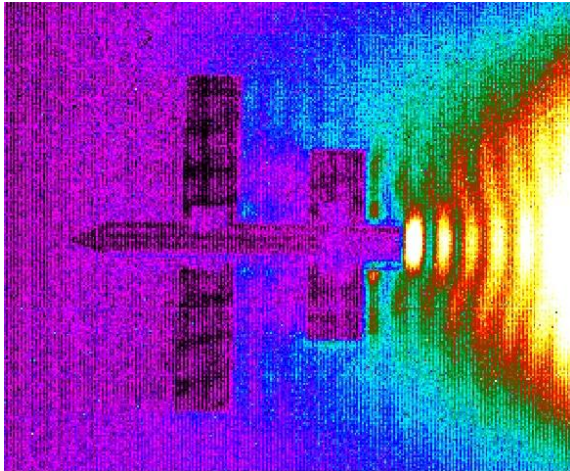
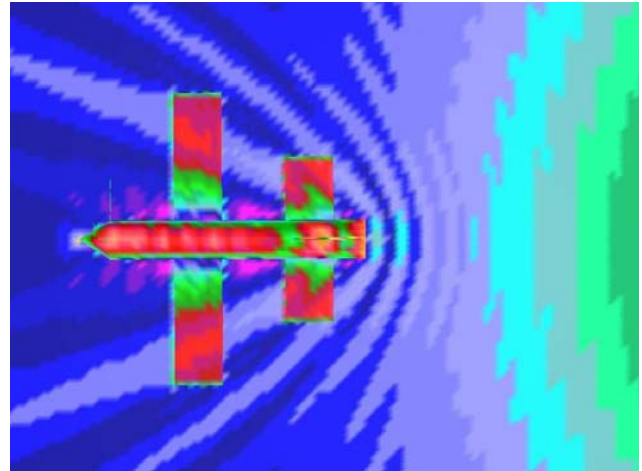


Figure 4. Nose-On at 6GHz (Incident Spherical Wave)
(a) Contour Map Showing Measured Relative Field Magnitudes Using the IR Technique, and
(b) Contour Map Showing Relative Co-Pole Field Magnitudes Using the CEM Simulation Technique



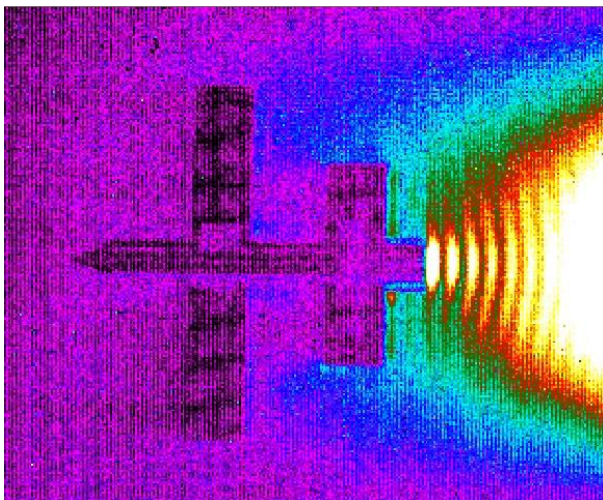
(a)



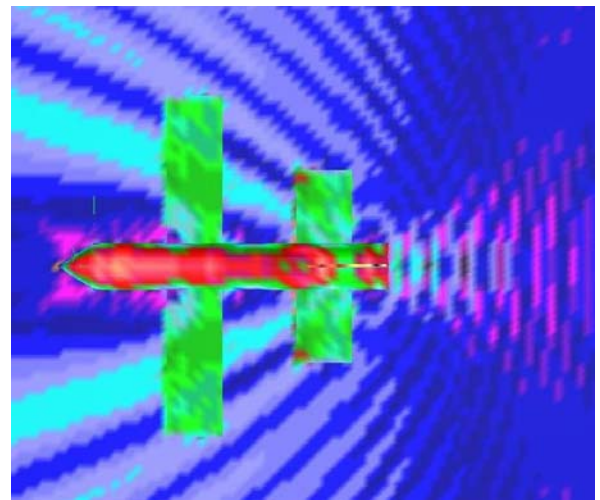
(b)

Figure 5. Tail-On at 4GHz (Incident Spherical Wave)

- (a) Contour Map Showing Measured Relative Field Magnitudes Using the IR Technique, and
 (b) Contour Map Showing Relative Co-Pole Field Magnitudes Using the CEM Simulation Technique



(a)



(b)

Figure 6. Tail-On at 6GHz (Incident Spherical Wave)

- (a) Contour Map Showing Measured Relative Field Magnitudes Using the IR Technique, and
 (b) Contour Map Showing Relative Co-Pole Field Magnitudes Using the CEM Simulation Technique

9.0 REFERENCES

- [1] J. D. Norgard and R. L. Musselman, "Direct IR Measurements of Phased Array Aperture Excitations," QIRT Journal, Vol. 2, No. 1, January 2005, pp.113-126.
- [2] J. D. Norgard and R. L. Musselman, "Direct IR Measurements of Phased Array Near-Field and Far-Field Antenna Patterns," QIRT Journal, Vol. 2, No. 2, July 2005, pp.223-236.
- [3] J. D. Norgard, R. Musselman, A. Drozd and I Kasperovich, "Validation and Verification of CEM Field Prediction Techniques Compared to IR Images of EM Fields for Complex Systems," 28th Annual AMTA Meeting & Symposium, Austin, TX, 24-26 October 2006, CD Conference Digest.